Morphological and morphometric assessment of the encephalic ventricles using different neuroimaging techniques

Article *in* European Journal of Anatomy · January 2012

Source: OAI

6 authors, including:

Juan A Juanes
Universidad de Salamanca
281 PUBLICATIONS 2,435 CITATIONS
SEE PROFILE

Alberto Prats-Galino
University of Barcelona
304 PUBLICATIONS 4,740 CITATIONS
SEE PROFILE

Morphological and morphometric assessment of the encephalic ventricles using different neuroimaging techniques

J.A. Juanes[1,2], M.J. Velasco[3], A. Prats[4], J.M. Riesco[1,2], E. Blanco[1,2], M. de la Fuente[5], J. Carretero[1,2], J. Delgado[6], M. Rubio[1,2] and R. Vázquez[1,2]

1,2- Dpto. Anatomía Humana e Histología Humanas e Instituto de Neurociencias de Castilla y León, Facultad de Medicina, Universidad de Salamanca, Salamanca, Spain

3- Servicio de Radiodiagnóstico, Hospital "Río Hortega", Valladolid, Spain

4- Dpto. de Anatomía y Embriología Humana, Facultad de Medicina, Universidad de Barcelona, Barcelona, Spain

5- Clínica Ruber, Madrid, Spain

6- Dpto. Psicobiología y Metodología CC, Facultad de Psicología, Universidad de Salamanca, Salamanca, Spain

Summary

An exhaustive analysis of the morphology and morphometry of the encephalic ventricles has been carried out using an array of diagnostic imaging techniques; namely, ultrasound, computerised tomography, magnetic resonance and its three-dimensional variant. The study was conducted on a total of 822 patients ranging in age from birth to 89 years old.

The incorporation of these techniques into the field of Human Anatomy has permitted researchers to gain a different and updated view of the anatomical structures present in living human beings. Thus, using ultrasound the ventricular system was identified in the form of sonolucent or anechoic areas. With computerised tomography, the ventricles appeared as hypodense images within the adjacent cerebral parenchyma. With magnetic resonance, and three-dimensional reconstruction, the ventricular morphology was visualised on the three spatial planes. Visualisation of the ventricular cavities by MR varied depending on whether they were enhanced in T1 or T2, or in proton density.

From the morphometric point of view, the cerebral ventricles exhibited variations in size that were directly related to the age of the patient; thus, age is a determinant factor in ventricular size. However, note should be taken of the low morphometric variability seen in IVv with respect to age. Regarding the other cerebral ventricles, size did depend on age.

Key words: Encephalic ventricles – Morphology – Morphometry – Neuroimaging

Introduction

The current importance in the field of diagnostic examination of the different radiological techniques available, together with the applications given to these in medical practice, demands that we should address the issue of assessment and the possibilities that these methods offer in the field of the morphological sciences, in particular in the field of Human Anatomy, as complements to the morphological information that can be gained from cadaver dissection. In this way it should be possible to broaden our knowledge of the anatomy of the different organs of the human body through use of currently available imaging techniques.

Submitted: January 30, 2003
Accepted: April 25, 2002

Correspondence to:
Prof. J.A. Juanes Méndez. Dpto. Anatomía e Histología Humanas, Facultad de Medicina, Avda. Alfonso X El Sabio s/n, 37007 Salamanca, Spain. E-mail: jajm@usal.es

Advances in diagnosis through the use of imaging techniques have revolutionised the world of conventional radiology. However, it is perhaps in the sphere of neurological diseases where the contributions of other diagnostic techniques, such as ultrasound, computerised tomography (CT) and magnetic resonance (MR), have found greatest relevance, not only owing to their very high resolution and definition but also, and especially, owing to their non-invasive nature.

Recent years have witnessed extraordinary advances in neuroradiology, such techniques being applied to the study and diagnosis of pathologies of the central nervous system (Raz et al., 1987; Mirvis, 1989; Leira et al., 1992; Gualdi et al., 1993; Wahlund, 1996; Matsumae et al., 1996; Cohen et al., 1998, among others).

The current reliability of these techniques, together with the possibility of direct visualisation of the nervous tissue itself and their sensitivity and specificity as regards a considerable number of pathological processes has led them to being the basis of today's diagnostic procedures. In this sense, radiological analysis of the structures of the brain is useful for locating atrophic or space-occupying lesions. It also allows situations involving obstructions to the circulation of the cerebrospinal fluid (CSF) to be detected.

Many pathologies of the brain structures have direct or indirect repercussions on ventricular morphology (Jeringan et al., 1982; Goldstein et al., 1986; Raz et al., 1987; Sacher et al., 1990; Kroft et al., 1991; López et al., 1995). These alterations can only be assessed by different diagnostic imaging techniques or at post-mortem, when cadaver biopsies are undertaken.

Although many processes affect the morphology of the cerebral ventricles, most of the literature consulted does not refer to how these areas of the brain are modified from the anatomo-radiological point of view.

From this viewpoint, few studies have made a joint assessment –using different diagnostic imaging techniques simultaneously– of the morphology and morphometry of the cerebral ventricles (Walser and Ackerman, 1977; Brassow and Baumann, 1978; Rottenberg et al., 1978; Penn et al., 1978; Pentlow et al., 1978; Pakkenberg et al., 1989; Naidich et al., 1989; Zipursky et al., 1990; DeCarli et al., 1992; Seidel et al., 1996; Celik et al., 1995; Heshavan et al., 1995). Accordingly, our aim in the present work was to gain deeper insight –using ultrasound, CT, MR, and three-dimensional reconstructions obtained with MR– into the anatomy of the cerebral ventricles by means of a descriptive and interpretative analysis of the anatomo-radiological images obtained with such techniques.

Thus, our aim was to perform a detailed analysis of the morphology and morphometry of the cerebral ventricles using different imaging techniques with a view to later identifying and interpreting normal anatomical pictures and possible variants.

Material and methods

A group of 822 patients with ages between 1 day and 89 years was studied. To collect ultrasound images of the brain structures of interest, we used a model RT-3000 ultrasound device from General Electric. The study was conducted on 248 individuals (Table 1) who, after exploration, were considered normal; the individuals' ages ranged between the first few hours of life and 9 months. For this ultrasound study we used the fontanelles as natural "windows", the anterior fontanelle being the structure most frequently used. On some occasions we employed the squamous part of the temporal bone, since in children this is still very thin.

Table 1.- Number of patients in the ultrasound study.

Age range (months)	Males	Females	Total
<1- 3	69	53	122
4-6	48	34	82
7-9	20	24	44

The *morphometric parameters* analysed were as follows:

For the *lateral ventricles* (LV):

- Distance between frontal horns (DFH)
- Distance between LV (collateral trigone) (DLV)
- Width of frontal horn (WFH)
- Width of LV body (WLVB)
- Distance from LV to cerebral cortex (DLVCC)

For the *Third or median Ventricle (IIIv):*

- Size of roof of IIIv (antero-posterior direction) (SR*IIIv*)
- Distance from roof to apex of IIIv (cranio-caudal direction) (DRA*IIIv*).

For the *Fourth Ventricle (IVv)*:

- Longitudinal axis (Long.)
- Transversal axis (Trans.)

In the case of CT, we used a *SOMATON-CR* device, from Siemens, on a total of 574 patients (Table 2) with ages ranging between one year and 89.

Table 2.- Number of patients in the CT study.

Age range (months)	Males	Females	Total
1-10	38	30	68
11-20	20	22	42
21-30	28	22	50
31-40	40	40	80
41-50	34	30	64
51-60	36	38	74
61-70	46	40	86
> 70	60	50	110

All patents subjected to this exploration were placed in the supine position with a headrest provided with a pillow so that the imaging would be centred and the patients would not move during the exploration.

On some occasions, if patients were agitated they were given light sedation or anaesthesia.

Once the patients were in position, a *topogram* was performed (similar to a lateral shot of the cranium) in which an oblique line passing through the base of the skull, with an angle between 8 and 14º, was traced.

Sections of 4 mm were taken every 4 mm at the base of the skull and 8mm/8mm in the rest of the skull up to the superior part of the cranium.

The patients were explored by X-rays beamed from a tube moving around them. These X-rays crossed the structures under study and formed the slice to be examined, being attenuated on the basis of their absorption coefficients.

The *morphometric parameters* analysed are shown in Scheme 1 and were as follows:

- Width of body of LV (WBLV) (1)
- Distance between external edges of the bodies of the LV (DEEBLV) (2)
- Width of frontal horns (WFH) (3)
- Width of occipital horns (WHO) (4)
- Distance between frontal horns (DFH) (5)
- Distance between occipital horns (DOH) (6)
- Width of third ventricle (WTV) (7)
- Transverse axis IVv (TAIVv) (8).

The central trend and the dispersion of the data, grouped in intervals, was analysed using conventional procedures performed through programmed routines on an Excel spread sheet. The specific formulas employed were as follows:

a) for the mean: $\bar{Y}=\frac{\sum n_i Y_i}{n}$

b) for the standard deviation: $S_y=\sqrt{\frac{\sum n_i (Y_i-\bar{Y})^2}{n}}$

Scheme 1.- Representation in axial sections of the morphometric parameters analysed by CT: Width of body of LV (1); distance between external edges of the bodies of the LVs (2); width of frontal horns (3); width of occipital horns (4); distance between frontal horns (5); distance between occipital horns (DOH) (6); IVv transverse axis (8).

c) for the estimator of the standard deviation of the mean:

$$\hat{}_{\bar{y}} = \frac{S_y}{\sqrt{n\text{-}1}}$$

in which:

n_i= frequency corresponding to each score;
Y_i= individual score (cms)
n= number of cases per age interval.

The corresponding data were explored using graphic analyses carried out with the DeltaGraph program, version 5.0. Graphics were constructed of 3D areas (age intervals•measurement(cms)•frequency), together with graphics of the means with error intervals: mean±standard deviation, and mean ± $z_{(95\%, /2)}$ •estimator of the standard error of the mean. This latter type of graphic can be used as a conventional procedure for the inferential analysis of the differences between the measurements of the age groups, with an error rate of 5% (Graphics 1-6).

The exploration with MR was carried out on a partial sample of 220 patients who required complementary exploration out of the total number used for the exploration with CT (574 patients) and who, after study, were considered to be normal.

A Toshiba MRT-50A device with a magnetic flux density of 0.5 teslas (1 Tesla= 10,000 Gauss) was used.

The patients were placed in the supine position on the exploration bed. A skull antenna (Brain QD) was placed around their heads. The patients were then introduced into the gantry, making every effort to ensure they would be at the centre of the magnetic field. Two scout images were taken of the location of the zone to be studied, one of them axial and the other sagittal, thus marking the exploration sequences.

To study the cerebral ventricles, sequences in the sagittal projection, *spin-echo* enhanced in T1, and in axial projection, *spin-echo* enhanced in T1/T2 (PD, proton density) and T2 were made. At the same time, 3-D reconstructions of the encephalic ventricles were made for individual study on the different spatial planes.

Results

Using the *ultrasound technique*, the ventricular system was readily identified in the form of sonolucent or anechoic areas. The images of the lateral ventricles were observed in coronal (Fig. 1a) and parasagittal (Fig. 1b) sections, as well as in axial sections (Fig. 1c).

In *coronal sections*, the lateral ventricles adopted a triangular shape at the level of the frontal horns (Fig. 1), whereas the ventricular body took on a semicircular aspect in relation to the choroid plexuses, which appeared as highly echogenic structures (Fig. 1a).

The parameters of the LV analysed in coronal sections pointed to the existence of morphometric variations that depended on the age of the individual, the values increasing in direct relation to this variable (Graphic 1).

The width of the frontal horns in the groups of patients with ages ranging between less than one month to three months had a mean of 0.14 cm (standard deviation, SD=0.10), the values ranging between zero, indicating that sometimes it could not be observed, to 0.43 cm (SD=0.14) as a maximum value, which was only seen in 8 patients.

In the subjects between 4 and 6 months of age, this parameter increased by 0.2 cm, therefore affording a mean of 0.36 cm (SD=0.12), and a maximum value of 0.6 was observed. The highest WFH value was seen in the group with ages between 7 and 9 months, the mean being 0.43 cm (SD=0.14).

The distance separating both horns ranged between 2.05 cm (SD=0.21) and 2.88 cm (SD=0.28), increasing in direct proportion to the age of the individual and with an observed maximum of 3.3 cm.

In *parasagittal sections*, the frontal horns, the body, and the collateral trigone were observed as sonolucent areas (Fig. 1b, d), together with the occipital horns, although with lesser clarity.

In one *axial* section, in the area of the frontal horn the LV were observed as an arch-shaped sonolucent area, as in the coronal section (Fig. 1).

The structures situated in relation to the lateral ventricles such as the caudate nucleus and the thalamus (Fig. 1b, e, f) were visualised with a medium degree of echogenicity.

Other structures such as the germinal matrix and the choroid plexuses were seen to exhibit very high echogenicity.

With ultrasound, in a *coronal* section (Fig. 1f) the third ventricle had the shape of a narrow cleft free of echoes, between the thalamus and the hypothalamus of the right and left cerebral hemispheres, which displayed a medium degree of echogenicity.

The morphometric values of the IIIv, analysed by ultrasound, are shown in Graphic 2. The size of the roof of this ventricle ranged in sagittal sections between a mean of 0.73 cm (SD=0.08) and 1.12 cm (SD=0.14) from the youngest time of life to 9 months, respectively.

In view of the short transverse extension of the IIIv, its ultrasound visualisation on a sagittal section plane required a very precise orientation of the image plane. In this situation we identified

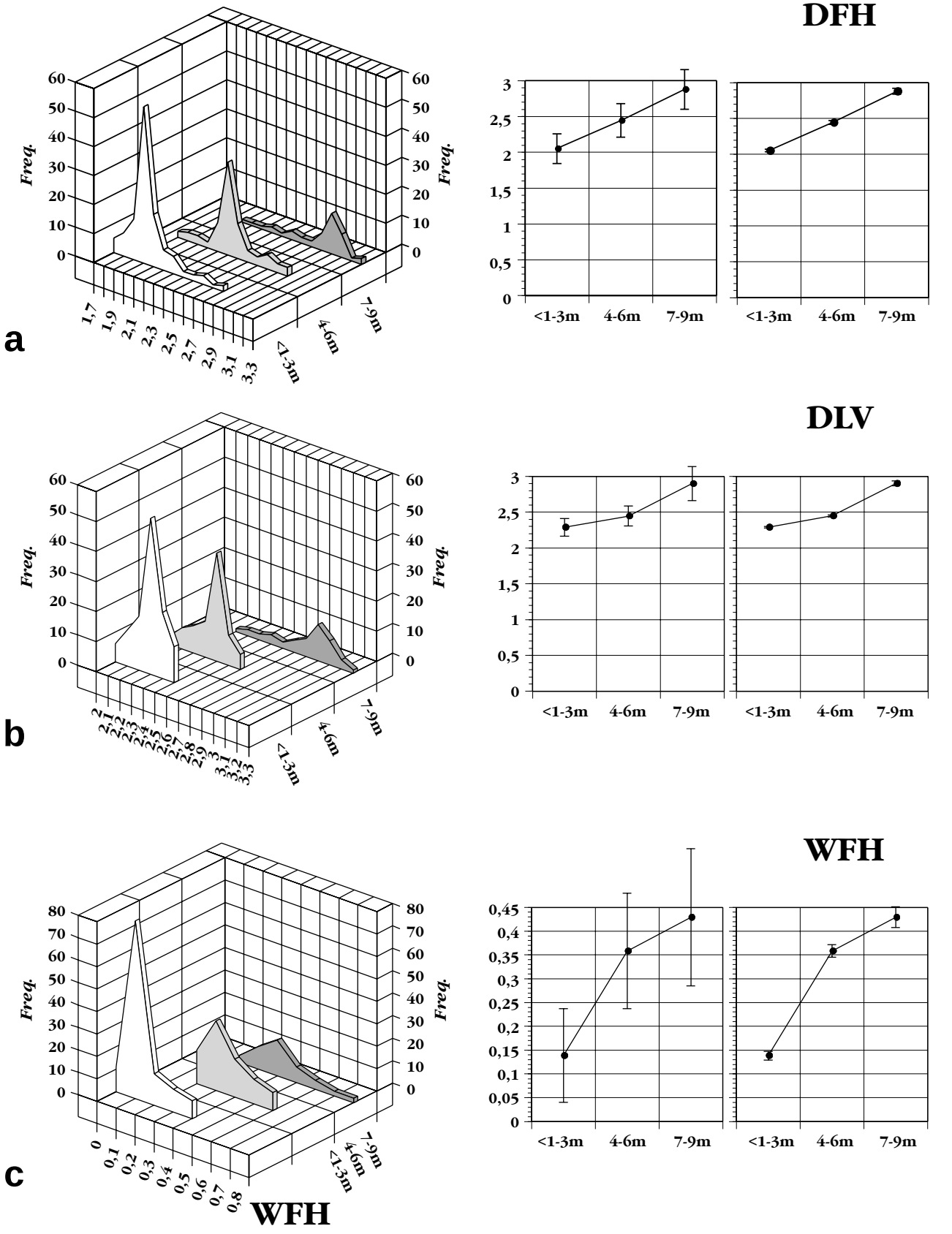

Graphic 1.- Ultrasound study. Frequency distribution of the mean values found for the following parameters in the lateral ventricles (LV). **a**: Distance between frontal horns (DFH); **b**: Distance between LV (collateral trigone) (DLV); **c**: Width of frontal horn (WFH). Values are expressed in cm.

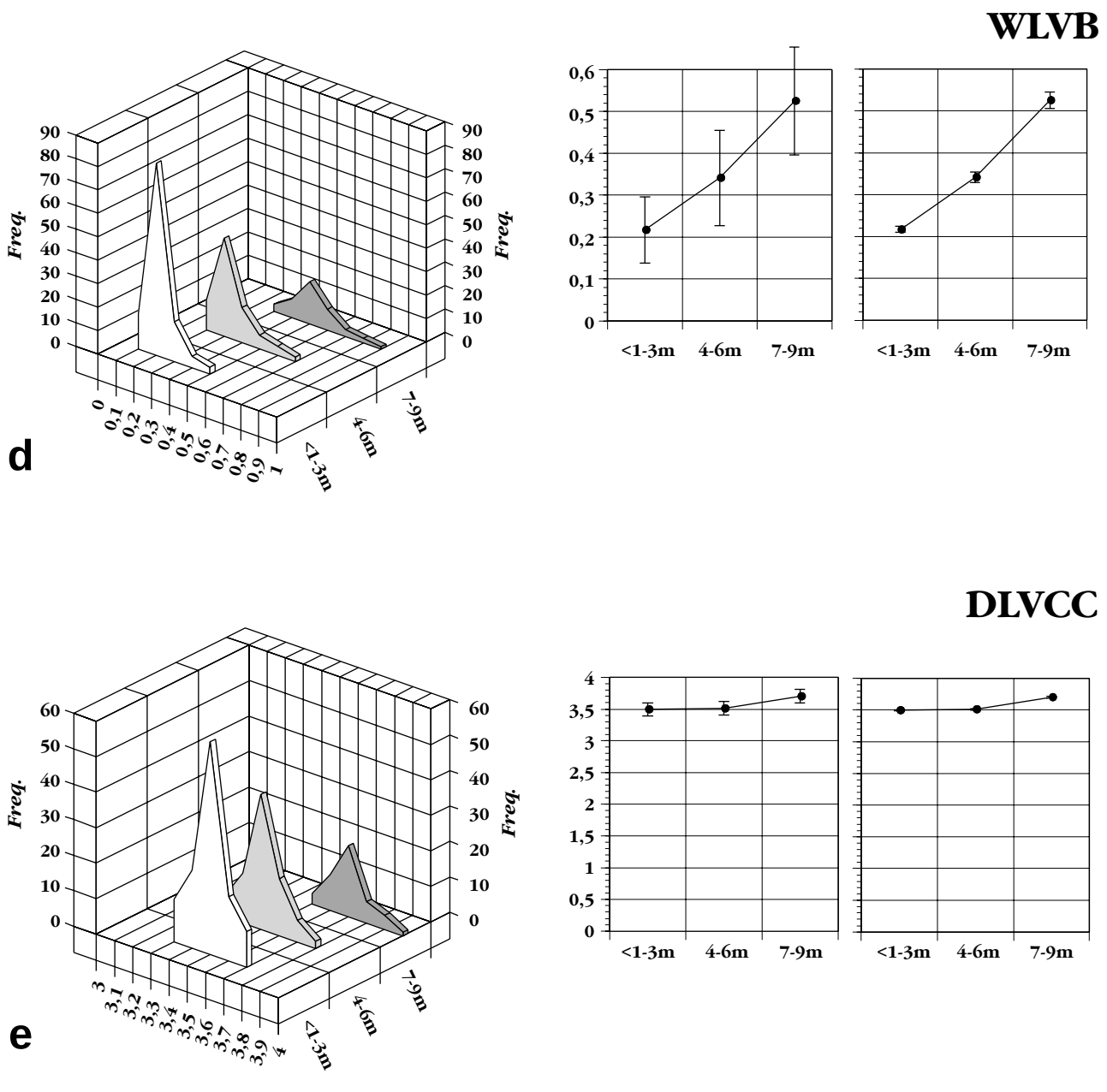

Graphic 1.- Ultrasound study. Frequency distribution of the mean values found for the following parameters in the lateral ventricles (LV) (cont.). **d**: Width of LV body (WLVB); **e**: Distance from LV to cerebral cortex (DLVCC). Values are expressed in cm.

IIIv well as an area of very complex contours, without echoes, and with a relatively large surface area. (Fig. 1d). Such complexity in its contours is due to the many anatomical structures limiting it, forming different recesses (Fig. 1d).

The best image of the IVv in ultrasound terms was obtained with a sagittal section. Behind the rhomboid fossa there was an anechogenic area, triangular in shape, which delimited the echogenic cerebellar vermis in a "tent-like" fashion.

The morphometric parameters of the IVv explored in sagittal sections (Graphic 3a) showed that the longitudinal axis of this cavity had a mean of 0.30 cm (SD=0.05), that of the other groups of patients considered increasing very slightly, with means of 0.36 cm (SD=0.10) and 0.39 cm (SD=0.07) respectively.

On the same section plane, the transverse axis of the IVv had a mean of 0.30 cm (SD=0.06) in patients between <1 to 3 months of age, and 0.37 (SD=0.10) and 0.41 (SD=0.07) respectively in the two older groups (Graphic 3b).

In *coronal* sections IVv appeared as an anechoic image, with an oval shape, centred on the posterior fossa.

Computerised tomography revealed the ventricular cavities with great clarity owing to the density of the CSF contained within them (Figs. 2 and 3). Although this technique mainly allows

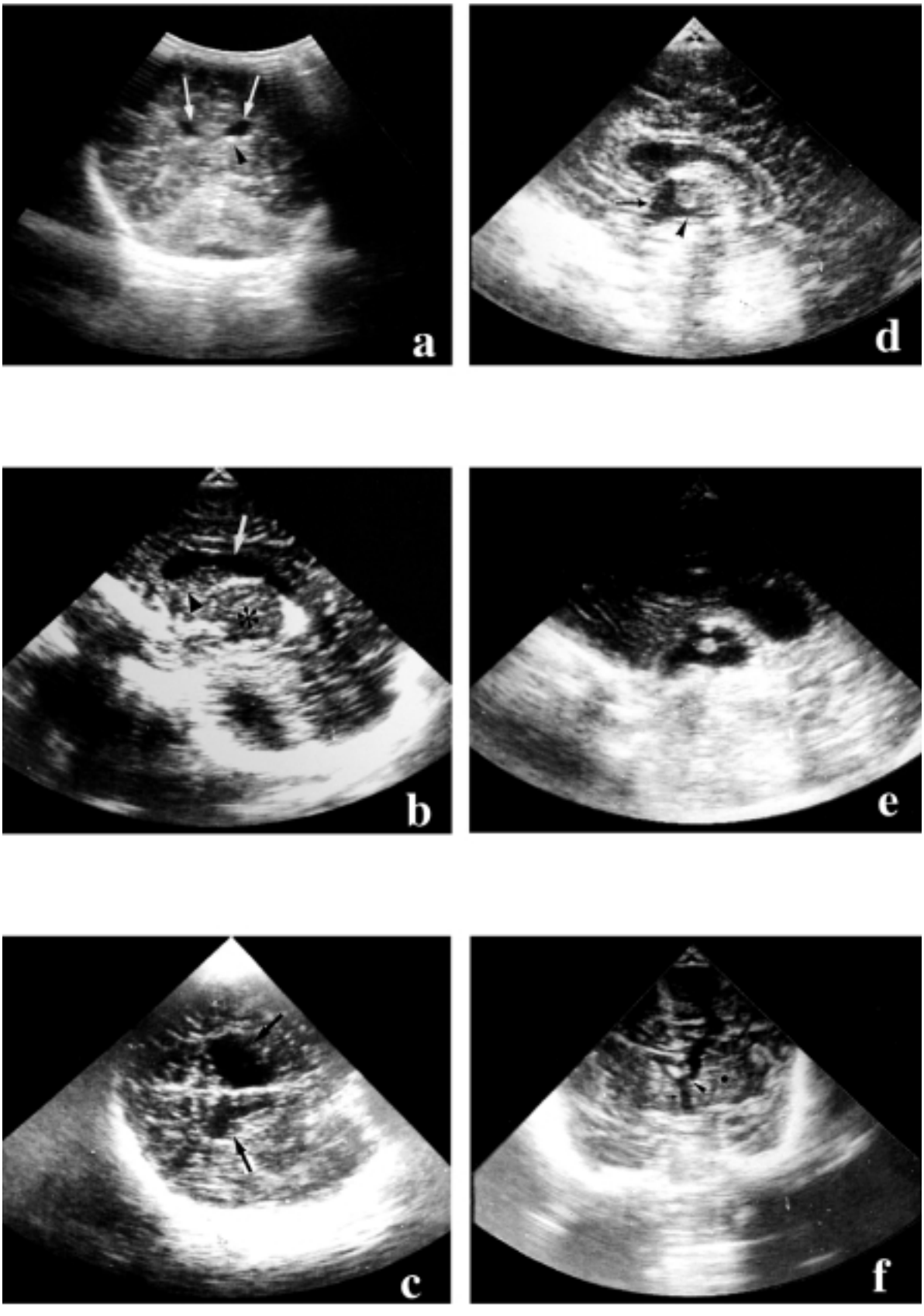

Figure 1.- *Ultrasound images.* **a:** Transfontanellar coronal section showing two highly echogenic images corresponding to the choroid plexuses (arrowhead) in relation to some anechoic linear areas corresponding to the lateral ventricles (arrows). **b:** Parasagittal section in which the lateral ventricle (arrow) can be identified as an anechoic or sonolucent image in the shape of a C. Below the frontal horn is the caudate nucleus (arrowhead), slightly echogenic, separated from the thalamus (asterisk) by an echogenic line corresponding to the thalamocaudate sulcus. **c:** Axial section at the level of the orbito-meatal line, obtained through the temporal bone. Note the presence of two anechoic structures with a triangular morphology (arrows) corresponding to the lateral ventricles, separated by the strongly echogenic interhemispheric fissure. **d:** Sagittal section showing the IIIv (arrow) and the posterior recess (arrowhead). **e:** Sagittal section of the IIIv clearly showing the highly echogenic intermediate mass. **f:** Coronal section in which a sonolucent image corresponding to the IIIv (arrow) and the thalamus (asterisk) can be seen, together with the union to the lateral ventricle through the interventricular foramen (arrowhead).

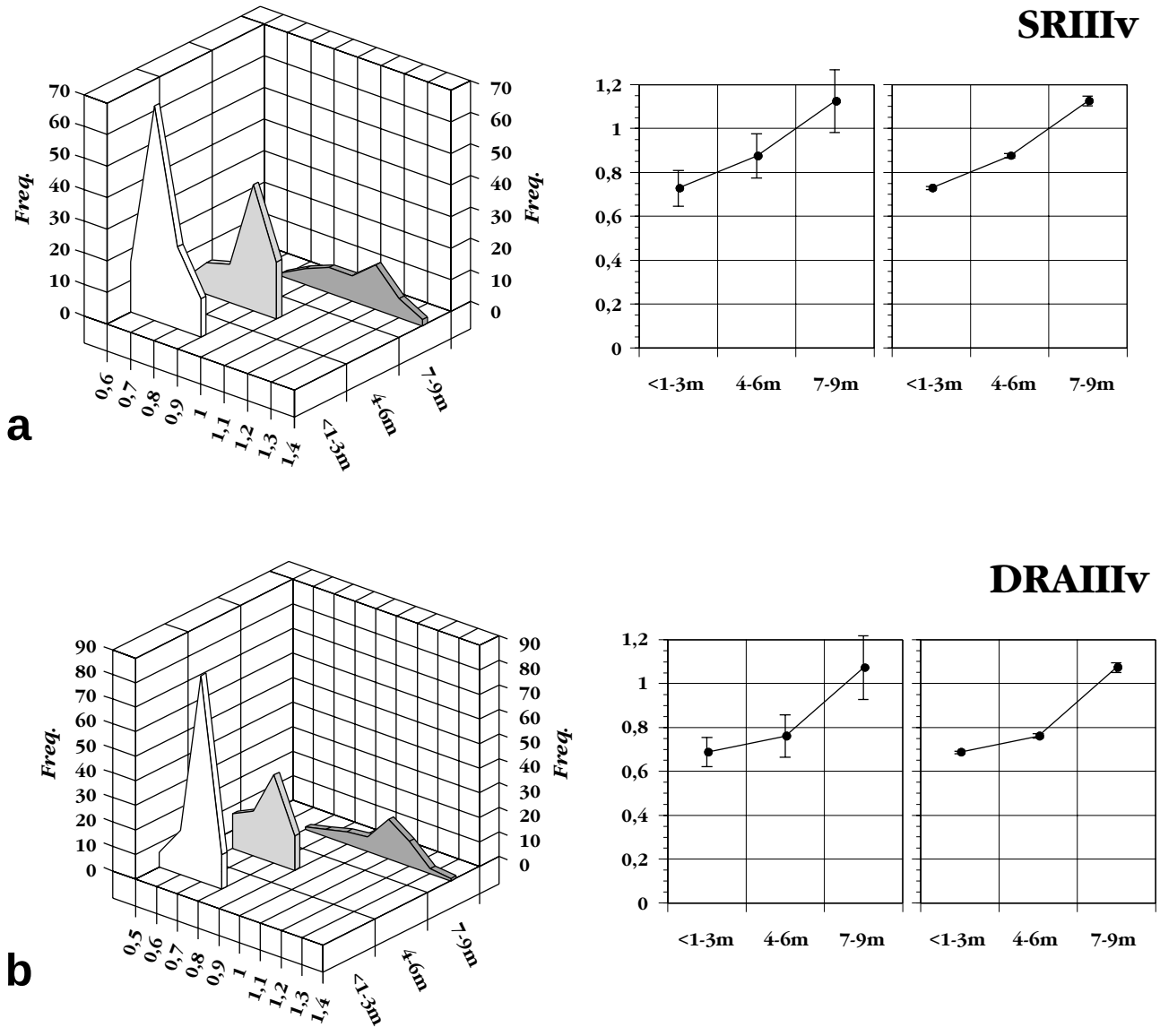

Graphic 2.- Ultrasound study. Frequency distribution of the values found for the following parameters in the third ventricle (IIIv). **a**: Size of roof of IIIv (antero-posterior direction) (SRIIIv); **b**: Distance from roof to apex of IIIv (cranio-caudal direction) (DRAIIIv). Values are expressed in cm.

one to obtain axial sections, on some occasions we performed multiplane reconstructions on the other two spatial planes -i.e., coronal and sagittal, as may be seen in Figure 3. In these, the cerebral ventricles appeared as hypodense images between the adjacent cerebral parenchyma. Nevertheless, the visual quality of the image was always poorer than in axial sections.

Despite the foregoing, with *magnetic resonance* (Figs. 4 and 5) the *three-dimensional reconstructions* made with this technique allowed us to observe the ventricular morphology on the three spatial planes –axial (Fig. 4a, b, c), sagittal (Fig. 4 d, e, f) and coronal (Fig. 5a-d)– and to "extract" the whole ventricular volume in isolation for joint three-dimensional assessment (Fig. 6).

Visualisation of the ventricular cavities with MR varied according to whether T1, T2 or proton density (T1/T2) was enhanced. Thus, with images enhanced in T1 the cerebral ventricles afforded a low signal (Fig. 5), whereas those enhanced in T2 gave a very high signal intensity, as seen in Figure 4c. Proton density revealed ventricular images of medium signal intensity (Fig. 4b).

According to CT analysis, the size of the ventricles varied from one individual to another, depending on their age, as seen in graphics 4, 5 and 6.

Using *axial* sections obtained with CT, the *lateral ventricles* were visualised as low-density cavities located on each side of the mid-line (Fig. 2). In MR sagittal sections of these ventricles, it

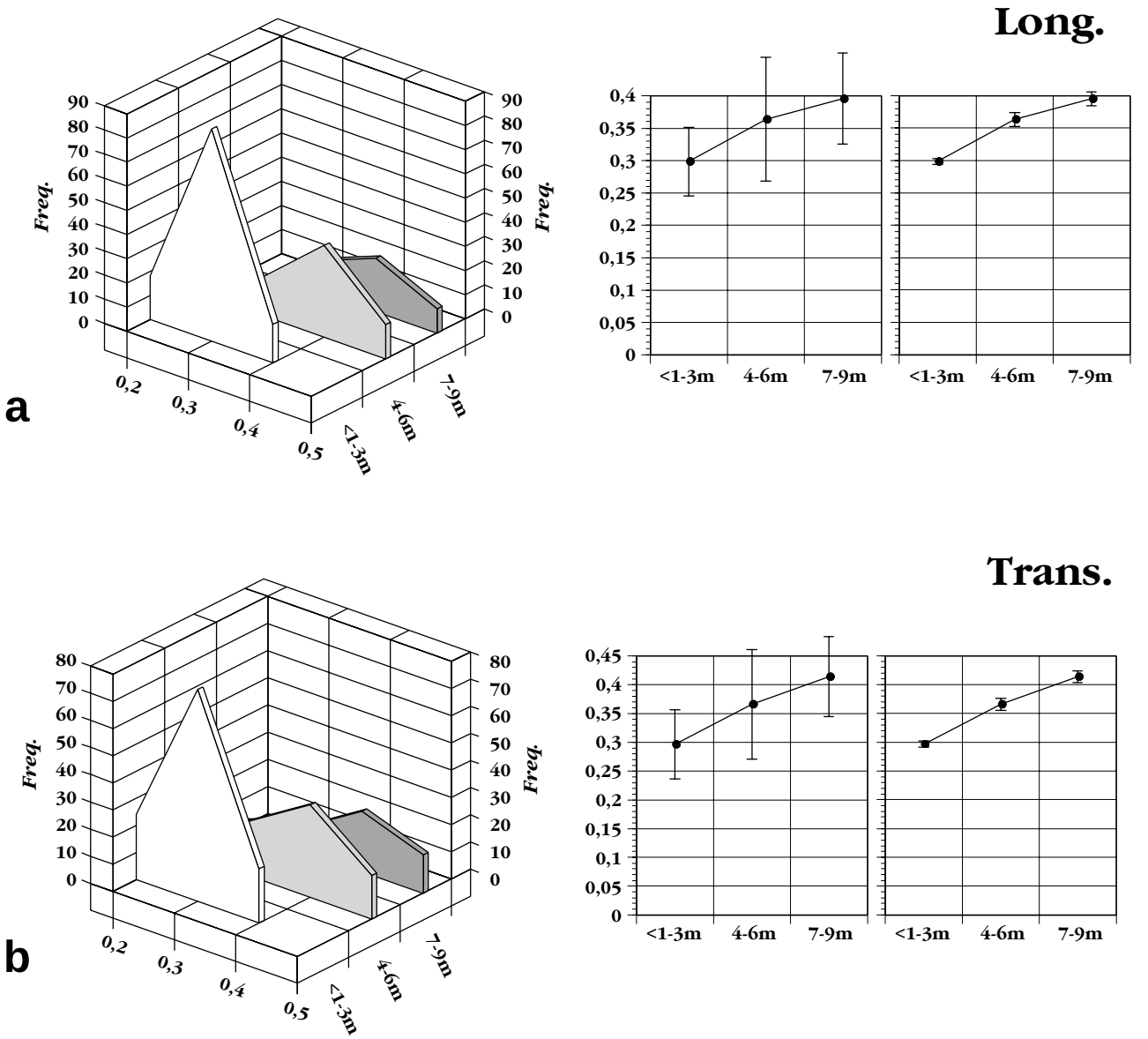

Graphic 3.- Ultrasound study. Frequency distribution of the values found for the following parameters in the fourth ventricle (IVv). **a**: Longitudinal axis (Long.); **b**: Transversal axis (Trans.). Values are expressed in cm.

was possible to observe their longitudinal extension from the frontal lobe to the occipital lobe (Fig. 4d-f). From the point of view of their reciprocal relationships, in coronal sections obtained with MR the lateral ventricles were seen to be separated from one another, maintaining individual communication with the median/third ventricle through Monro's foramen (Fig. 5b).

Three-dimensional reconstruction with magnetic resonance allowed assessment of the lateral ventricles (Fig. 6). Thus, from the frontal lobe the lateral ventricle first coursed backwards to the posterior end of the optic thalamus. There, it changed direction and coursed downwards and forwards, ending at the anterior end of the temporal lobe (Fig. 6). In this last part of its trajectory, the lateral ventricle successively surrounded the posterior end of the optic thalamus and the inferior face of the cerebral peduncle. Finally, at the point where it changed direction, the ventricle sent a horizontal and curvilinear diverticulum to the posterior end of the brain; this diverticulum seemed to prolong its original direction backwards (Fig. 6).

In both the axial sections obtained with CT and MR and in the MR sagittal sections and their 3-D variant, we describe three portions in the lateral ventricle:

- An anterior or *frontal* portion (Figs. 3a, 4d, 5a, 6a), extending from the anterior end of the ventricle to the posterior part of the optic thalamus;
- A posterior or *occipital* portion (Figs. 2b, 5d, 6c,d,e), extending through the occipital lobe from the posterior part of the optic thalamus;

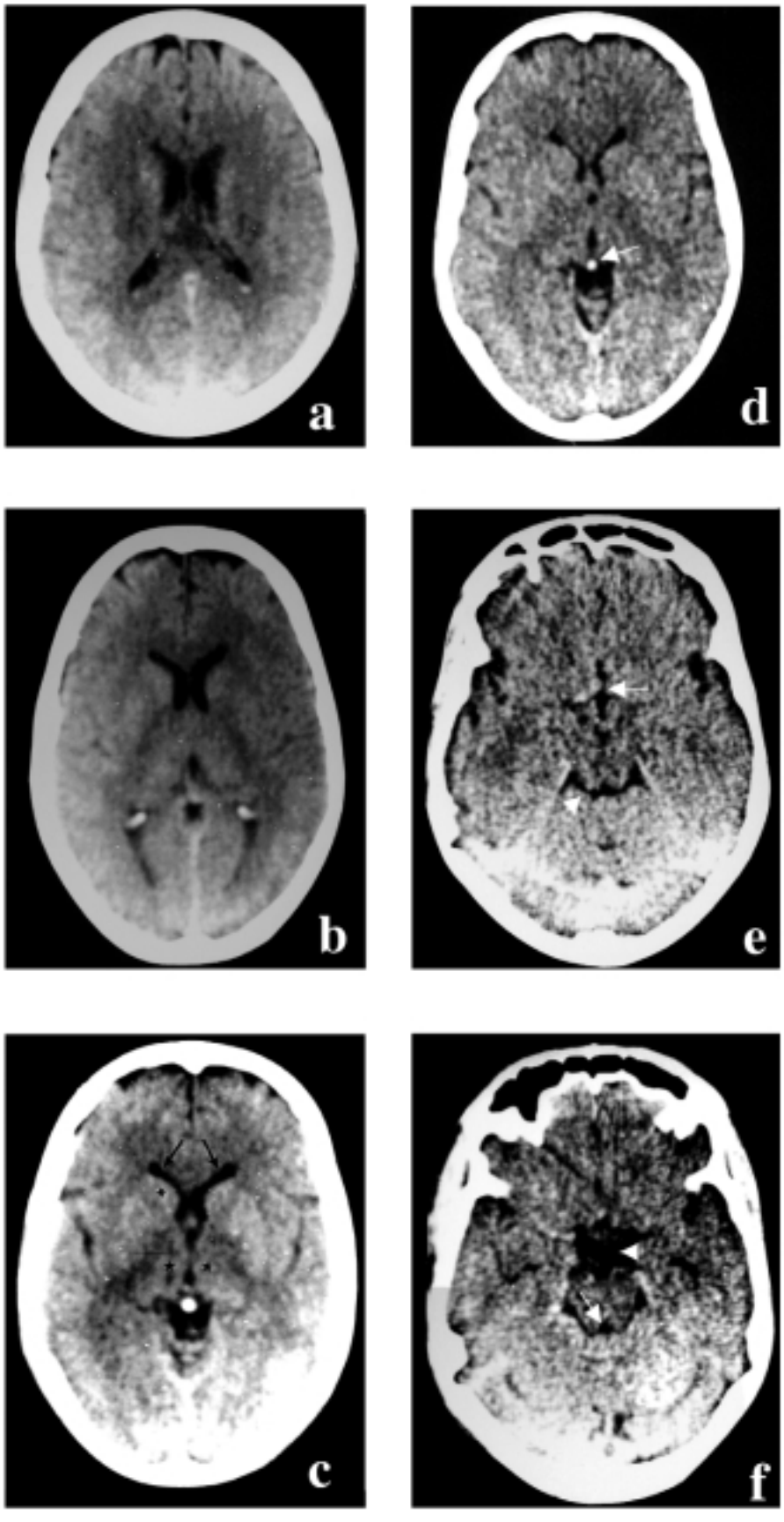

Figure 2.- Axial sections, in the cranio-caudal send of CT, in which the hypodensity of the encephalic ventricles can be seen with this diagnostic imaging technique. **a:** Transverse section at the level of the body of the lateral ventricles; the zone of greater density within the ventricles correspond to the choroid plexuses. **b:** Tomographic section showing the frontal and occipital horns of the lateral ventricles. Note hypodensities in the zone of the collateral trigone. **c:** Visualisation of the frontal horns of the lateral ventricles (arrows); on the infero-external edge it is possible to observe the caudate nucleus (asterisk) with the same density of soft parts. In the central part of the section is the IIIv, delimited by the thalamic nuclei (stars). **d:** Section at the level of the frontal horns of the lateral ventricles and the third ventricle, with hypodense characteristics. In the posterior part is the highly hyperdense calcified pineal gland (arrow). **e:** Tomographic section taken at the level of the IIIv (arrow). The quadrigeminal cistern is in the posterior part (arrowhead). **f:** Section at mesencephalic level, showing the Sylvian aqueduct (arrow) and the basal cistern (arrowhead).

- An inferior or *temporal* portion (Figs 4e,5c, 6c,d), encompassing the descending portion of the ventricular cavity.

The three portions came together at the posterior part of the thalamus, forming the collateral trigone (Fig. 5d), which was best seen with 3-D MR (Fig. 6c, d).

The body of the lateral ventricle coursed from forwards to backwards, describing a slightly convex curve towards the cranium (Figs. 4d, 6b, c, d). On average, the width of the body of the lateral ventricles ranged between 0.33 cm (SD=0.09) and 1.29 cm (SD=0.16), depending on the age of the individual (Graphic 4a).

The upper part, or roof, of the lateral ventricle, slightly concave in the posterior sense –as can be seen in the images obtained with 3-D MR (Fig. 6 c, f), was formed by the inferior face of the corpus callosum.

The inferior wall or floor extended obliquely downwards and inwards (Fig. 6).

On its external part, the floor displayed a mass, with dense soft parts according to CT, that was slightly denser than the corpus callosum and slightly protruding, corresponding to the caudate nucleus of the striate body.

The caudate nucleus afforded an image similar to that of a comma, both in the axial CT sections and in those obtained with MR; the thick end, or head, of this coursed forwards and its small end, or tail, became sharper and was prolonged backwards to the ventricular collateral trigone.

More medially to the caudate nucleus was the optic thalamus, a set of grey matter nuclei, with a density very similar to the caudate nucleus in the sections performed with CT (Fig. 2c), such that it was better differentiated in the MR images (Figs. 4 and 5).

The optic thalamus contributed to the formation of the lateral ventricle only through the external half of its superior face.

In coronal MR sections, between the anterior end of the optic thalamus and the part corresponding to the trigonum, it was possible to visualise Monro's foramen, which communicated the frontal portion of the lateral ventricle with the median ventricle (Fig. 5b).

The lateral edge of the trigonum, coursing obliquely forwards and inwards, was accompanied along its whole length by vascular tracts, corresponding to the choroid plexuses, with a tomographic density similar to that of neighbouring structures which on occasion were calcified, above all in the older individuals.

The *middle ventricular cavity* appeared as a single hypodense image in axial CT sections (Fig. 2e). It was very flattened and was located between the two optic thalami (as confirmed in the coronal sections obtained with MR), which to a large extent formed its lateral walls (Fig. 5b).

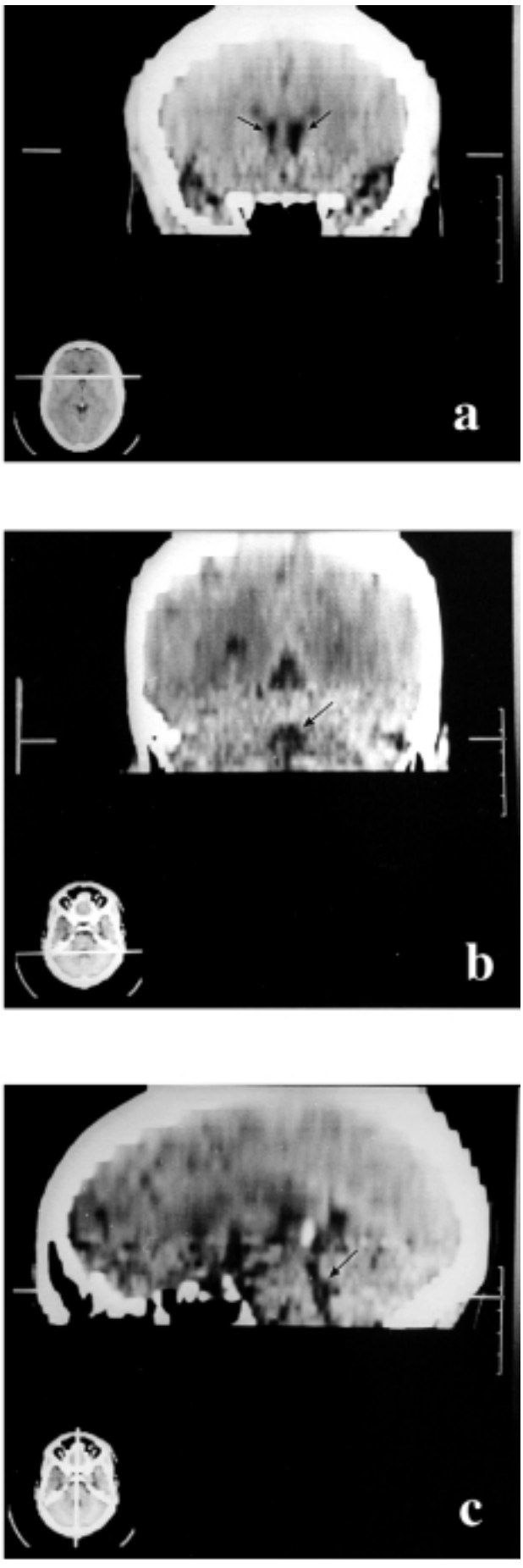

Figure 3.- Tomographic reconstructions in coronal (**a, b**) and sagittal (**c**) sections at the level of the frontal horns of the lateral ventricles (**a**) (arrows) and at the level of the fourth ventricle (**b, c**) (arrows).

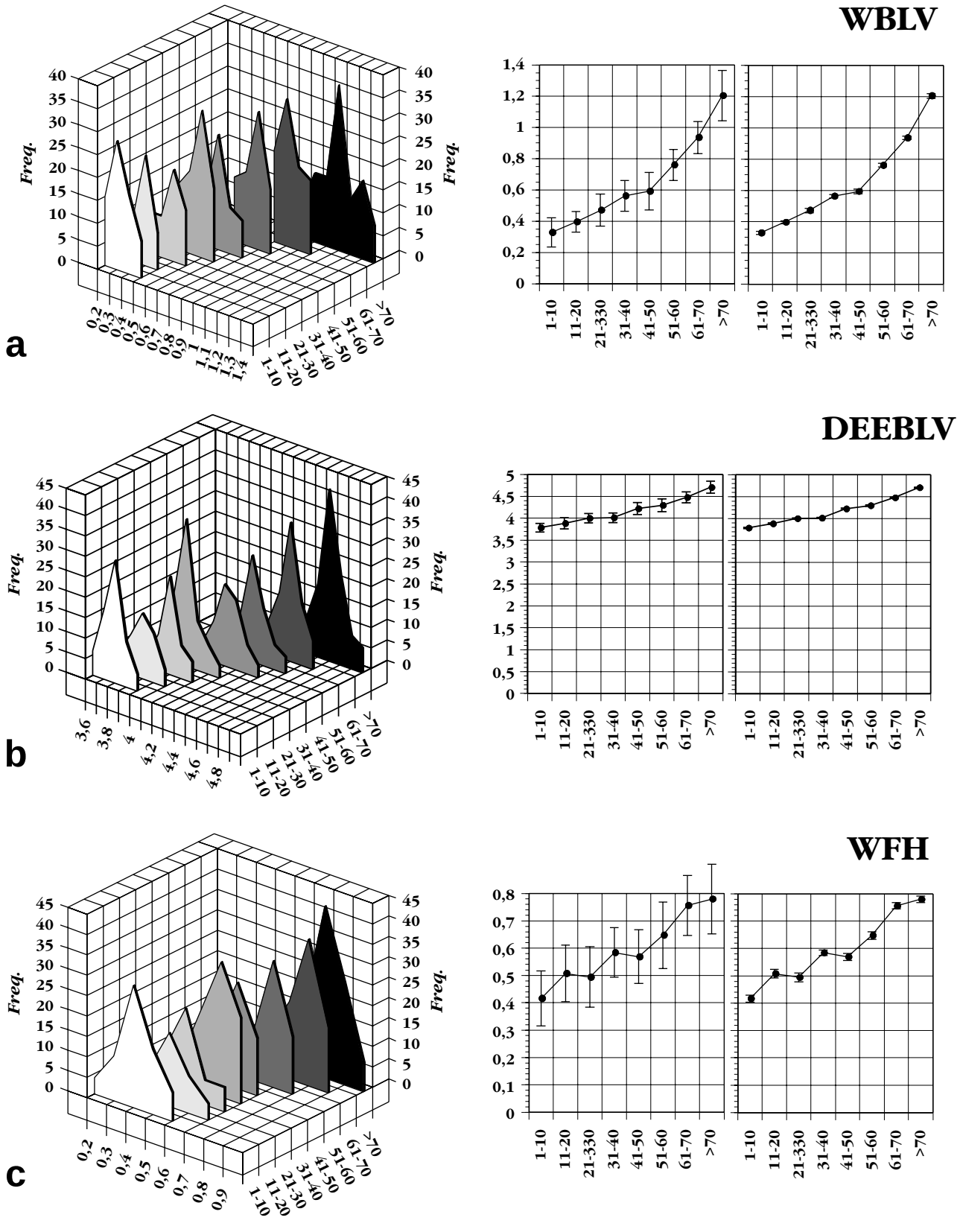

Graphic 4.- CT study. Frequency distribution of the mean values found for the following parameters in the lateral ventricles (LV). **a**: Width of body of LV (WBLV); **b**: Distance between external edges of the bodies of the LV (DEEBLV); **c**: Width of frontal horns (WFH). Values are expressed in cm.

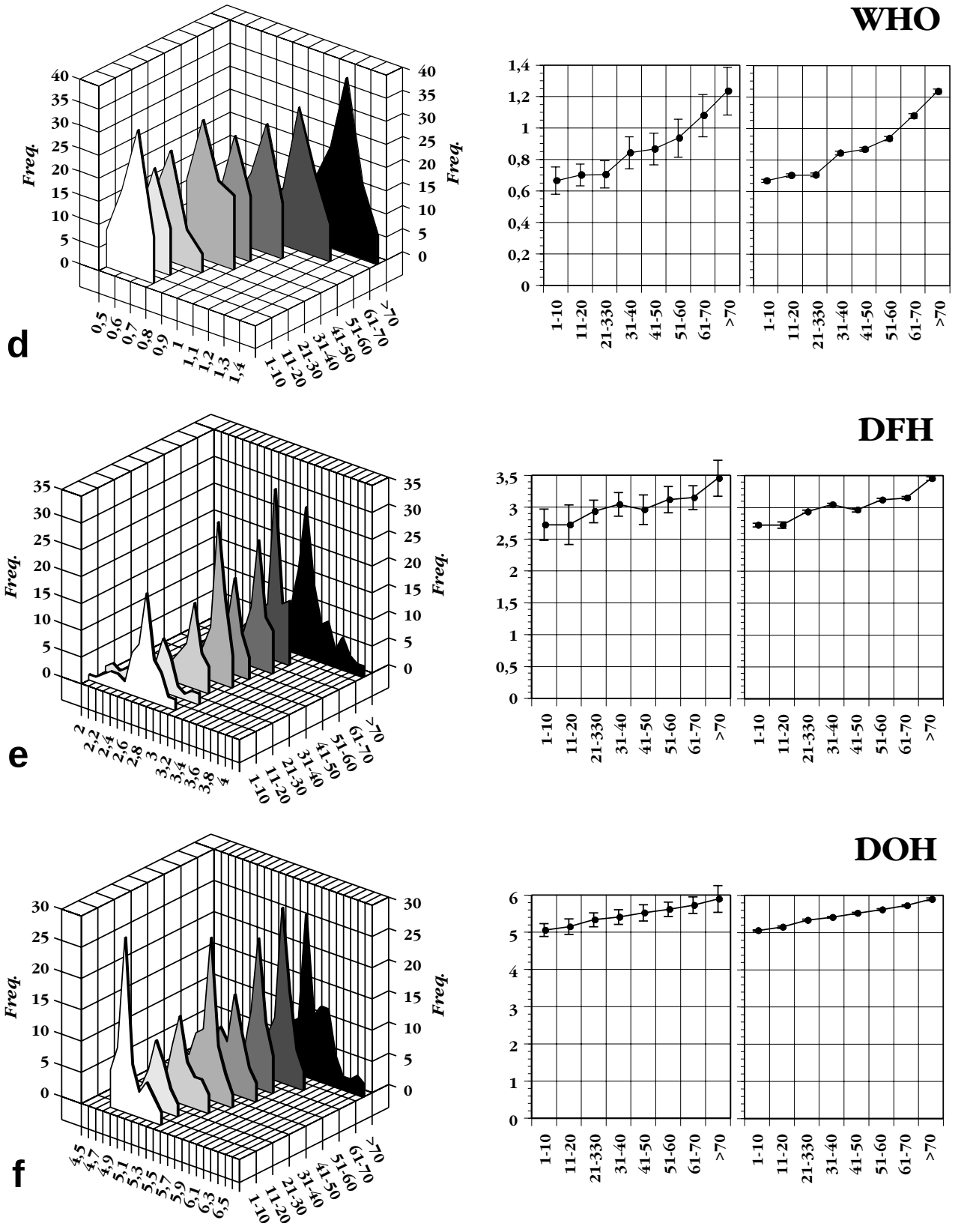

Graphic 4.- CT study. Frequency distribution of the mean values found for the following parameters in the lateral ventricles (LV) (cont.). **d**: Width of occipital horns (WHO); **e**: Distance between frontal horns (DFH); **f**: Distance between occipital horns (DOH). Values are expressed in cm.

The communication of the third ventricle with the fourth ventricle was very clear in the sagittal sections performed with MR (Fig. 4f).

The median ventricle was funnel-shaped, the base coursing upwards, and its sides were flattened in the transverse sense. These data could readily be explored in a sagittal section obtained with MR.

In the axial sections obtained with CT, we measured the width of the median ventricle, which ranged between 0.21 cm (SD=0.07)= and 0.80 cm (SD:0.10); an increase directly proportional to the age of the individual was observed (Graphic 5).

The superior portion strongly resembled an almond. Its major antero-superior axis was formed by the anterior two thirds of the internal face of the optic thalamus.

The posterior edge of the IIIv coursed downwards in an oblique direction. It was related to the pineal gland; the posterior white commissure, and the upper part of the two quadrigeminal tubercles (Fig. 4f).

The anterior edge of the IIIv coursed downwards and forwards, strongly approaching the vertical.

The apex of the IIIv corresponded to a funnel-shaped zone, appreciable in sagittal MR images (Fig. 4f). This zone coursed downwards and forwards, ending in a more or less sharp point in the superior half of the pituitary stalk.

The IIIv displayed a series of prolongations or recesses observable in sagittal MR images (Fig. 4f) and their 3-D variants (Fig. 6d).

Thus, in the thalamic portion it was possible to observe an anterior horn, between the two interventricular foramina. Behind, a posterior horn or suprapineal recess was seen (Fig. 4f), located above the orifice of the midbrain aqueduct.

In the tuberoinfundibular portion, an antero-inferior prolongation was observed; this was subdivided by the optic commissure into two recesses: the optic recess, in front, and the infundibular recess, behind (Fig. 4f).

The *fourth ventricle* (IVv) corresponded to the cavity located between the cerebellum, the medulla oblongata, and the protuberance. As in the ventricular cavities described above, it appeared as a low-density image in CT sections (Fig. 3b,c) and as an image of varying signal intensity, depending on the enhancement, with the MR technique (Figs. 4f, 5d).

The transverse axis of the IVv had a mean length of 1 cm, ranging between 0.91 cm (SD=0.07) and 1.06 cm (SD=0.10). These values varied slightly and not linearly with the age of the individual (Graphic 6).

The anterior wall of the IVv formed the floor of the ventricular cavity. Its major axis, located on the mid-line, coursed obliquely from top to bottom and from back to front. A transverse line, joining the two lateral angles, –i.e., the posterior-most parts of the lateral recesses– formed the minor axis and divided the floor into two triangles: one inferior, corresponding to the medulla oblongata, and the other superior, belonging to the protuberance.

The midbrain aqueduct was analysed in sagittal MR images (Fig. 4f) as a conduit that joined the third ventricle with the fourth ventricle. This conduit extended from the superior angle of the IVv to the dorsal portion of the mesencephalon. On average, in adults the length of the aqueduct ranged between 1.5 and 1.8 cm, although it was sometimes longer. Its diameter, observed in axial tomodensitographic sections, ranged between 1 and 2 mm.

This conduit of interventricular communication was narrower in the middle part than at its two ends, where its lumen adopted the form of a small curvilinear triangle.

Discussion

For many years, diagnosis by images has been based on the use of X-rays. Recently, however, it has been expanded thanks to imaging techniques based on alternative physical principles, such as ultrasound reflection, computerised tomography, magnetic resonance, isotope emission, etc. In imaging diagnosis, knowledge of anatomy has always been attributed a key role for understanding the research findings and for correct application of these in clinical practice. Accordingly, a complete knowledge of gross Anatomy allows researchers and physicians to take better advantage of the diagnostic possibilities of imaging techniques. Joint collaboration between anatomists and radiologists is very useful for morphological assessment of the different structures of the organism analysed from different points of view, unifying criteria that ratify the meticulous and exhaustive description of anatomical structures. Also, imaging techniques have received technological and scientific contributions from other branches of medicine, electronics, physics and mathematics. Conventional radiology has undergone significant changes, new diagnostic methods appearing every so often that are able to provide an increasingly accurate view of the anatomy of living beings. Thus, imaging diagnosis is currently a fundamental pillar in clinical medicine.

All these procedures have in common the reproduction, through images, of the normal and pathological anatomy of the organism, such that today the term radiology tends to be replaced by imaging diagnosis (Kirkwood, 1990). Although the concept of radiological diagnosis of brain structures is not new to radiologists and anatomists,

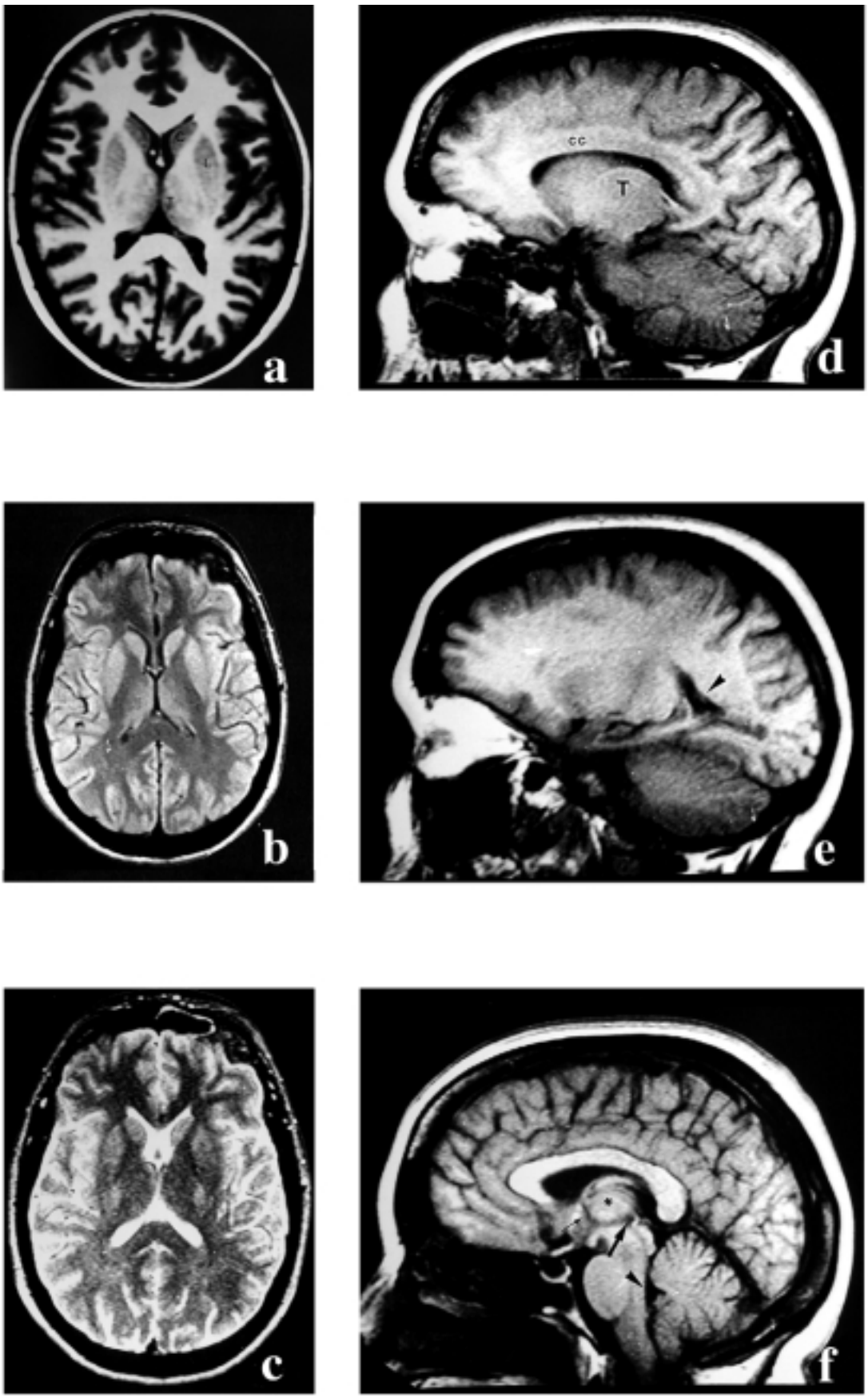

Figure 4.- Axial (**a, b, c**) and sagittal (**d**, **e, f**) MR sections. **a:** Axial section, enhanced in T1, showing the hypointense lateral ventricles (asterisk) and some periventricular nuclei such as the head of the caudate nucleus (C), the lenticular nucleus (L) and the thalamus (T). **b** and **c**: Axial sections enhanced in proton density (**b**) and the same section enhanced in T2 (**c**), showing the lateral ventricles with their hypointense and hyperintense prolongations, respectively. **d:** Parasagittal section enhanced in T1, showing the hypointense frontal horn of the lateral ventricle. Cranially, it is possible to observe the corpus callosum (cc) and, caudally, the thalamus is seen (T). **e:** Parasagittal section enhanced in T1 at the level of the collateral trigone (arrowhead), with hypointense characteristics. **f:** Sagittal section enhanced in T1, showing the IIIv (thin arrow), in relation to the thalamus (asterisk). On the posterior wall is the pineal recess (thick arrow), and the triangular morphology in the section of the encephalic IVv (arrowhead).

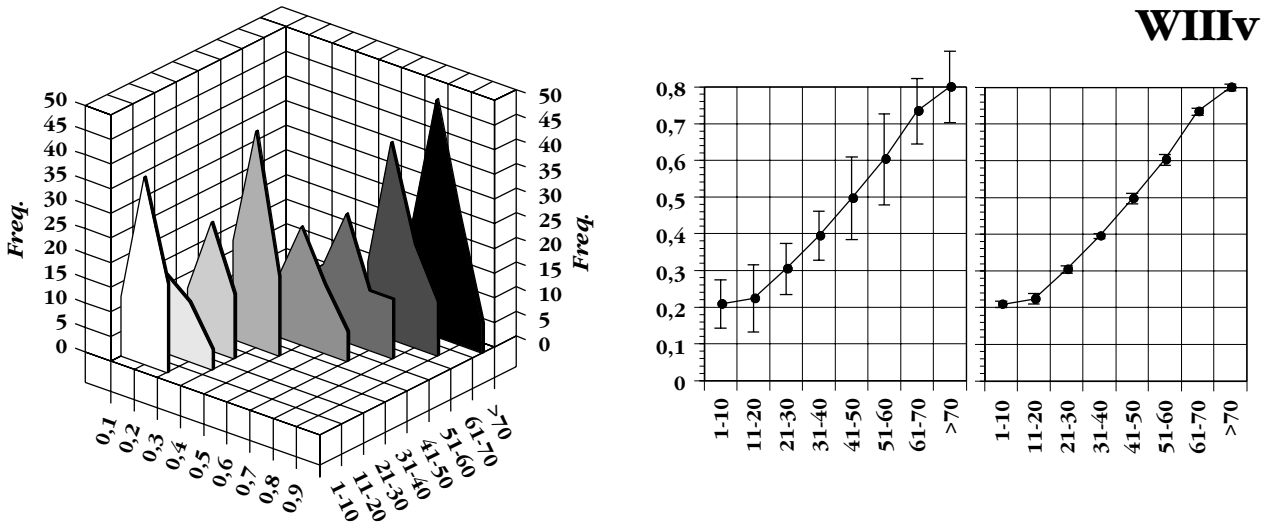

Graphic 5.- Frequency distribution of the values found for the width of third ventricle (WTV). Values are expressed in cm.

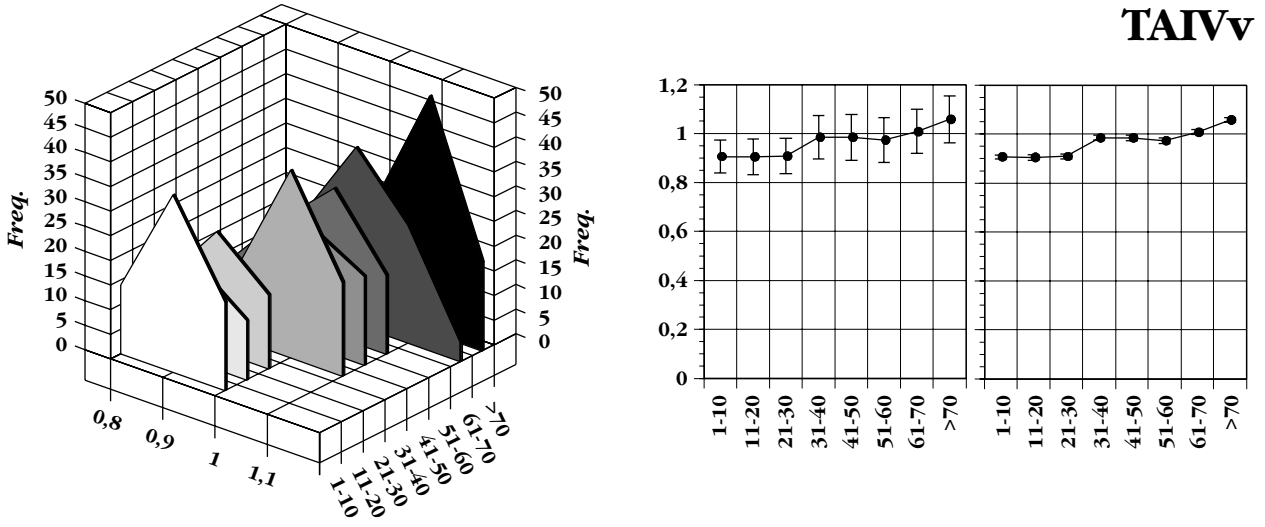

Graphic 6.- CT study. Frequency distribution of the values found for the transverse axis of the fourth ventricle (TAIVv). Values are expressed in cm.

there are few studies that have exhaustively addressed neuroradiology *via* currently available imaging techniques. Accordingly, the present work offers a detailed study of the radiological aspects of the normal anatomy of the cerebral ventricles, covering their description from the simplest techniques to the more modern ones of three-dimensional reconstruction.

Ultrasound exploration has mainly been used to study the encephalon of newborns and has found considerable application in recent years, to a large extent owing to increased demand from neonatology units and the appearance of high-resolution sectorial dynamic probes, which enable the bregma fontanelle to be used appropriately as an acoustic window (Jeanty et al., 1981; Dewbury and Bates, 1981). Initially, static exploration was used but this was discontinued after the advent of dynamic probes, owing to the ease with which it is possible to explore newborns in the conscious state, with no restraints. This is almost impossible with the manual technique, although it afforded optimum results for another author (Kremkau, 1980). Another disad-

vantage of static exploration is the impossibility of observing the pulsations of the intracranial vessels, an important anatomical reference for assessing neighbouring structures.

One positive aspect of sectorial dynamic study is the possibility of exploring children even while they are still in an incubator (Grand et al., 1981). However, the ideal situation for satisfactory exploration is that the newborns should be calm and that the small movements of the probe and the slight pressure exerted should not alarm them. In our explorations, these aspects were always taken into account.

The most important sections to be made are the coronal ones, with different inclinations of the probe with respect to the orbito-meatal plane, and sagittal ones, with different degrees of obliqueness. The former are obtained by swinging the transducer backwards and forwards and ensuring that the underlying structures remain symmetrical with respect to the mid-line.

For study of the normal brain, the fact that the child is lying down –whether face up or face down– or not does not have much importance and it may well be suitable to have it sitting in its mother's lap (very comfortable for both) since sectorial probes are very easy to handle (Pigadas et al., 1981).

In our study, the ease with which we were able to individualise the lateral ventricles and adjacent anatomical structures allowed us to observe rapidly whether our explorations were correct and whether the amplification curve was the most appropriate one.

According to ultrasound visualisation, the many anatomical structures of the brains of newborns can be better individualised when they are referred to images obtained with the sectorial probe. Accordingly, in our study we employed coronal and sagittal sections with different degrees of inclination and we pinpointed the structures to be studied on these images.

The cerebral ventricles were readily visible owing to their anechogenicity, accompanied at the level of the lateral ventricles by the high echogenicity of their posterior wall owing to the presence of the choroid plexuses.

The structure of the lateral ventricles is perhaps what is defined and recognised soonest in the newborn brain. Their lateral limits appear precisely and their shape is unequivocal. In them, it is possible to visualise the choroid plexuses as highly echogenic structures; they are lengthened in shape and have a cotton wool-like aspect. They course throughout the lateral ventricle, with the exception of the frontal horns.

Authors such as Chitkara et al. (1988) have reported that the choroid plexuses appear between the 6th and 7th week of gestation: first in the roof of the fourth ventricle, then in the lateral ventricles, and finally in the third ventricle. Towards the 9th week, the choroid plexuses occupy almost 75% of the ventricular cavities; as from that time, they decrease in size in favour of actual ventricular growth.

The lateral ventricles develop strongly and are visualised very clearly between the 12th and 16th week of gestation. During the 2nd term of pregnancy, they occupy most of the cranial content, forming a well-defined symmetric image.

Jeanty et al. (1981) analysed the development of the ventricle/hemisphere ratio, relating this to gestational age. In a normal foetus, this ratio decreases progressively from 15 to 25 weeks, the decrease occurring most rapidly between the 15th and 24th week.

Studies carried out by Goldstein et al. (1988) on foetuses analysed the ratio between the amplitude of the frontal horns and gestational age; as gestation progressed, this ratio decreased.

Other readily recognisable structures in sectorial exploration were those corresponding to the cerebral arterial circle (of Willis), the main branches of the middle cerebral arteries in the Sylvian fissure, and also the anterior cerebral artery in its trajectory along the corpus callosum; this was because they appeared as pulsating areas. Likewise, beyond the lateral ventricles it was also easy to identify the third ventricle and Monro's foramen, which established communication between them. However, it should be take into account that the third ventricle is not recognised with precision until the 16th week of gestation (Gilmore et al., 2001).

As seen in the ultrasound images obtained by us, the median ventricle was represented by a linear, anechoic image. It was flanked on both sides by the thalamus and, in front, by the *septum pellucidum* and in the posterior part by two symmetric, hypoechoic images corresponding to the cerebral peduncles. These findings were seen in coronal sections while in sagittal sections the third ventricle was represented by a triangular image pointing downwards.

In the medial sagittal sections, it was also possible to observe the IVv, the midbrain aqueduct, and neighbouring structures, in front of the mesencephalon, that were relatively echogenic, such as the pons and the medulla oblongata, which were immediately below and behind the cerebellar vermis, which was more echogenic. Nevertheless, we should like to stress that only in a very meticulous exploration of the posterior part of the cerebral peduncles is it possible to observe a central zone, a small point-like echo corresponding to the midbrain aqueduct. Usually, the aqueduct is not visible, and is only seen in dilation studies.

At times after the second term of pregnancy it was relatively easy to observe the fourth ventricle in both axial and sagittal sections. It is not

easy to recognise the IV ventricle in usual explorations of the foetus via coronal sections; it is usually identified in pathological situations, such as certain cases of hydrocephaly, but only when medial sagittal sections are taken. Other structures readily seen in coronal sections, apart from the cerebral fissures (interhemispherical, Sylvian, etc), were the cerebral peduncles, the thalamus and the caudate nuclei.

Among the advantages to be gained from the use of ultrasound is the fact that the method is non-invasive, is portable, inexpensive and does not emit radiation. Thus, it can be used to make repeated examination of the brain on several planes (Ellington et al., 1982; Hagen-Ansert, 1989). Neuro-ultrasonography is therefore the first choice diagnostic technique for the first months of life, the anterior fontanelle being a sufficiently large acoustic window for visualization of the brain structures (Beno-Ora et al., 1980; Cremin et al., 1983). Despite this, in some intracranial pathologies, such as cerebral oedema, subarachnoid or subdural haemorrhage, tumours or alterations in myelinization, the images obtained with CT or MR are in general more useful than those obtained with ultrasound.

Explorations made with the colour echo-Doppler technique incorporate data on the vascularisation of the brain, analysing flow in the arterial and venous vessels and hence permitting a reliable diagnosis in cases of cerebral ischaemia or haemorrhage, and aneurysms, which lead to an increase in vascular resistance in the cerebral parenchyma of the territory affected.

Computerised tomography represents one of the most significant advances in imaging diagnosis after the discovery of X-rays for neuroradiology (Baker, 1975; Evens, 1976). In neuroradiology, CT has led to a qualitative change of such magnitude that currently it is difficult to even conceive of the speciality without the contribution of this technique (Ambrose, 1973; Lanksch and Kazner, 1976).

With conventional radiology it is possible to discriminate four densities of grey, corresponding to soft tissue, fat, bone and metal. By contrast, with CT more densities can be analysed, expressed in attenuation units (Hansfield units (HU)). Because the numerical density of water ranges between +10 and -10 HU, and since the intraventricular CSF displays an aqueous density, this allowed us to perform a tomographic assessment through its hypodensity, thereby enabling us to assess ventricular morphology and morphometry.

The morphometric values analysed by us can be compared with those of other authors, using different imaging diagnostic techniques (Gyldensted and Kosteljanetz, 1976; Denkhaus and Winsberg, 1979; Synek et al., 1979; Cramer et al., 1990; Aylward and Reiss, 1991; DeCarli et al., 1992; Shah et al., 1992; Jonson et al., 1993; Celik et al., 1995; Keshavan et al., 1995; Bandiera et al., 1996; Tang et al., 2001).

Since different authors used different diagnostic techniques, in some cases the values differed slightly from our own results. Notwithstanding, in our series we wish to stress the high number of patients analysed with respect to the series reported above.

This technique permits different manoeuvres with the numerical matrix and anatomical images. Of great interest is the possibility of measuring the radiological density of the component structures of the image (Evens, 1976; Lanksch and Kazner, 1976; Huckman et al., 1977).

The high resolution of CT –both spatial and densitometric– is the product of certain basic principles that govern the system (Mancuso and Hanafee, 1985; Fleckenstein and Jensen, 1995). Among them, the following can be quoted:

a) The pronounced collimation of the beam of rays, which to a large extent limits secondary and disperse radiation. Depending on the width of the beam, which is regulated by collimation, the thickness of the slice explored varies; this may range from centimetres to millimetres.
b) The selective irradiation of a plane, without superposition of structures composing the neighbouring planes. In conventional tomography, the beam of rays passes through planes other than the one being studied, which produces parasite shadows on the recording of the stratum examined, with the consequent decrease in informative capacity.
c) Each plane explored is irradiated, around its whole perimeter, through the beam emitted by the tube, which turns from 180º to 360º around the patient. With 180 degrees, the time of duration of the section is reduced to half, although the information received at the computer is also reduced and the image reconstructed looses anatomical and densitometric resolution.
d) The availability of highly sensitive detectors, able to record small differences in the spectrum of the beam of X-rays emerging from the organism. The reconstruction of each slice is carried out on a matrix or grid formed by thousands of tiny equal-sized squares, each of which corresponds to an organic sector; the computer averages the coefficients of absorption of the X-rays of the tissues included in each square and assigns them a value, called the CT number. The overall set of these values forms a numerical matrix that is representative of the tomographic anatomical section, which

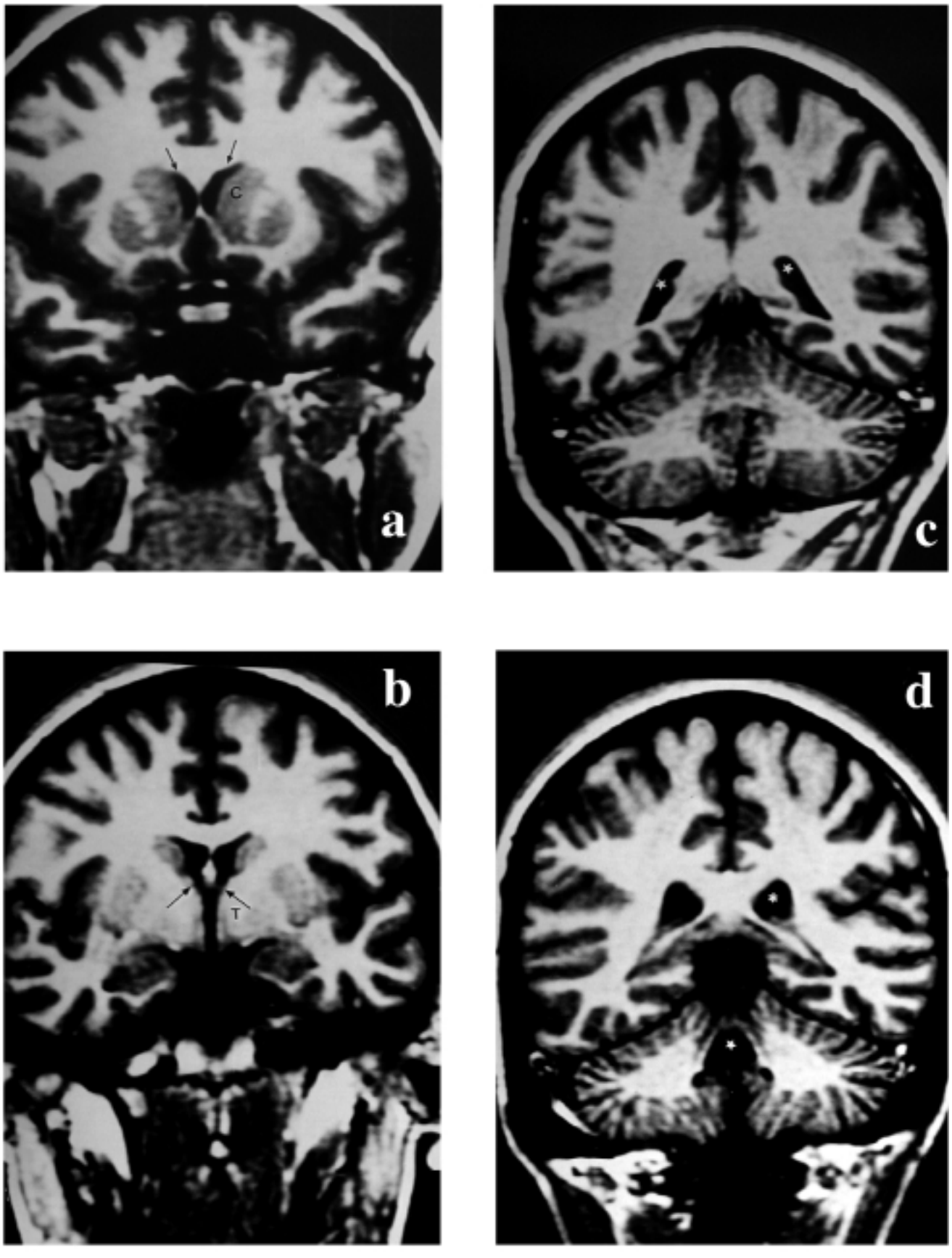

Figure 5.- Coronal or frontal sections with MR. **a:** Section enhanced in T1, showing the frontal horns of the lateral ventricles (arrows) in relation to the caudate nucleus (C). **b:** Section enhanced in T1 showing the frontal horns of the lateral ventricles joined to the IIIv by the interventricular foramen (arrows). Related to the thalamus (T) is the IIIv. **c:** Section enhanced in T1, showing the temporal prolongation of the lateral ventricles (stars). **d:** Section enhanced in T1 showing the zone of the collateral trigone (asterisk) and the fourth ventricle (star) in relation to the cerebellum.

is then converted into an image for correct diagnostic understanding and interpretation (Ambrose, 1973; Baker, 1975; Ambrose, 1977; Caird, 1977; Berninger et al., 1981).

With magnetic resonance, non-haemorrhagic organic fluids, such as the CSF, have long relaxation times (RT), giving hypointense images in T1 and hyperintense images in T2 with respect to soft tissues.

Proteins in aqueous solution decrease the T1 and T2 of water. Fluids such as abscess liquid have a shorter T1 than simpler fluids such as CSF. In MR images, this solution appears in the darkest part of the scale of greys. However, proteinaceous fluids show a moderate signal intensity that is quite difficult to differentiate from most soft tissues because they are iso- or hypointense in T1. By contrast, in images enhanced in T2 proteinaceous fluids have a high resonance signal, higher even than that obtained with urine or CSF (Brandt-Zawadski and Nornam, 1987; DeCarli et al., 1992).

The diagnostic potential of MR is based on organising the appropriate sequences and parameters to achieve a suitable contrast in the structures under study.

Assessment of the cerebral ventricles is feasible since the CSF, which occupies their interior, can be distinguished in both an image enhanced in T1, the black ventricle of the CSF being highlighted, and in images enhanced in T2, in which they are visualised as a very whitish colouration (DeCarli et al., 1992).

In general, explorations used to study the brain usually involve images enhanced in T1 and such images are therefore very morphological because the fluids appear in black, the white matter in white, and the grey matter in grey. They also use images enhanced in T2, which are very sensitive to pathological alterations, and images enhanced in proton density (D/P).

These three types of sequences were those used in our study, the images enhanced in T1 therefore being those with the greatest amount of information provided. However, the images that best served to detect pathological processes were usually T2, which are essential in all explorations with MR.

Where MR seems to have failed to live up to expectations is in specificity. Although MR is a very sensitive method, it is not very specific. It is able to obtain a high contrast in the soft parts, allowing an accurate delimitation of the extent of the pathology. Another drawback lies in exploration times, which for the time being are very long. All standardised studies comprise three main tomographic presentations (sagittal, coronal and transverse), together with two or three sequences of images of each section enhanced in T1, in T2 and in D/P. All this makes it necessary to use different parameters, thereby raising the costs of the test and rendering it susceptible to artefacts brought about by patient movements.

Explorations with MR have vary considerably in their duration; this difficult to typify and depends on the power of the magnetic field and the precision required. Most authors agree that a good average is one hour per patient. During this time, a sagittal scan is made in images enhanced in T1; an axial scan in images enhanced in DP, and a coronal scan in images enhanced in T2. To this time should be added the introduction of the sequences, prior calibration and on-screen visualisation of the images obtained (Young, 1984; Stark and Bradley, 1987; Kean and Smith, 1986; Jacobson, 1987; Muñoz González et al., 1989; Fleckenstein and Jensen, 1995).

In our study, all these exploration times and the collection of images were very prolonged since our work, although within the usual standardised exploration, focused on the precision of the sections selected and on their enhancement so as to obtain the best images and the best imaging information.

Finally, we should like to stress the following aspects of the neuroimaging techniques used in this study. Ultrasound is the method of choice during the first nine months of life, the anterior fontanelle being the ideal acoustic window for the visualisation of the ventricular structures –these being seen as anechoic images. The fact that it is user-friendly and has no secondary effects for the patient mean that it is the ideal technique for children younger than 12 months of age, and it can be used as many times as is necessary.

As from the first year of life, study of the cerebral ventricles is only feasible with CT and/or MR and its 3-D variant. However, the latter technique is optimum for overall anatomical assessments since it allows one to "extract" the whole ventricular volume and analyse it, in isolation, in any spatial position desired.

With computerised tomography, the cerebral ventricles are visualised owing to the low density of the CSF contained in them, and they appear as hypodense images within the surrounding parenchyma of the brain. This technique offers few advantages for morphological analysis of the ventricles, since although it is possible to perform reconstructions on the sagittal and coronal planes they are of low technical quality, and it therefore is axial sections that are made with this technique, thereby preventing precise analysis of these brain structures.

Magnetic resonance offered the best morphological data concerning the cerebral ventricles. Their visualisation varied, depending on the sequence employed. Thus, in images enhanced in T1 the cerebral ventricles appeared with low

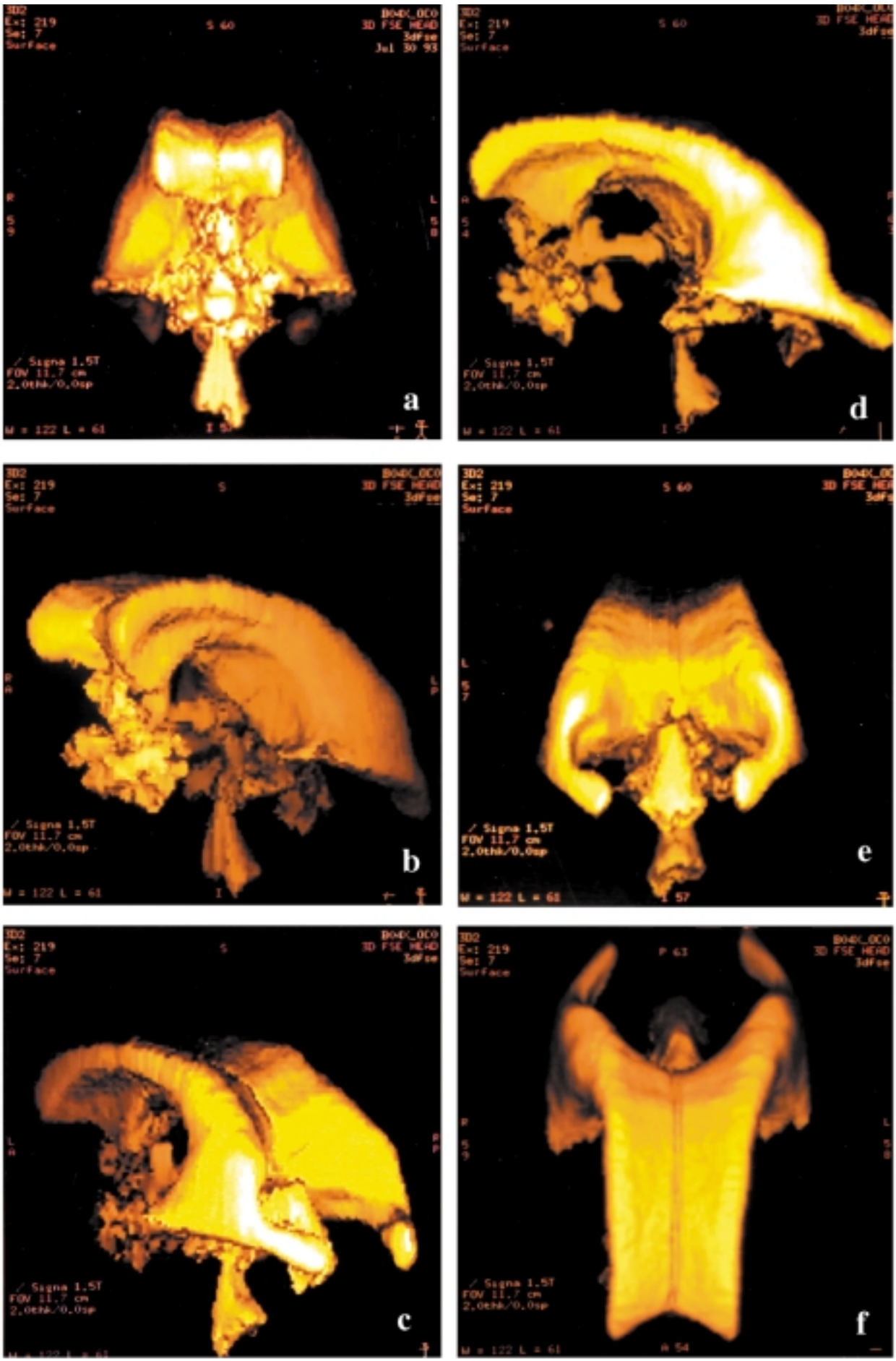

Figure 6.- Three-dimensional reconstructions of the ventricular mould with MR. Visualisation on different degrees of spatial rotation: **a:** anterior; **b:** antero-lateral; **c:** postero-lateral; **d:** lateral; **e:** posterior; **f:** superior.

signal intensity in black. In turn, in images enhanced in T2 the ventricles appeared with very high signal intensity and hence in white. Finally, in images enhanced in D/P the ventricles appeared with intermediate signal intensity between T1 and T2.

From the morphometric point of view, the cerebral ventricles showed variations in size that were directly related to the age of the individual. Thus, age must be a determinant factor in ventricular size. Nevertheless, we stress the low morphometric variability seen in the IVv with respect to age, the mean maximum value being 1.1 cm and the minimum 0.9 cm; in the other ventricles, size was age-dependent.

From the radiological point of view, knowledge of the anatomy of the cerebral ventricles in normal individuals can alert the physician as the occurrence of pathological processes, their size and exact topographic location, for later surgery or radiotherapy.

In conclusion, in this work we have attempted to offer some good imaging information of the cerebral ventricles in the hope of ensuring that the most appropriate imaging techniques will be used in the precise diagnosis of any lesion in the zone and that patients will be subjected to minimum discomfort, using the reference techniques rationally to explore each particular pathological process. The incorporation of these techniques to the field of Human Anatomy has allowed a different and updated view of the anatomical structures of living human beings.

References

Ambrose JAE (1973). Computerized transverse axial scanning (tomography): Clinical application. *Br J Radiol*, 46: 1023-1047.

Ambrose JAE (1977). Exploración con Tomografía Computada: Mirada Retrospectiva. *Seminarios de Roentgenología*, 12: 8-14.

Aylward EH and Reiss A (1991). Area and volume measurement of posterior fossa structures in MRI. *J Psychiatr Res*, 25: 159-168.

Bandiera P, Pirino A, Conti M, Achene A and Montella A (1996). Morphometric analysis of the lateral ventricles in living human. *Ital J Anat Embryol*, 101: 203-209.

Baker HL (1975). The impact of computed tomography on neuroradiologic practice. *Radiology*, 116: 637-640.

Ben-ora A, Eddy L, Hatch G and Solida B (1980). The anterior fontanelle as an acoustic window of the neonatal ventricular system. *J Clin Ultrasound*, 8: 65-67.

Berninger WH, Axel L, Norman D, Napel S and Redington RW (1981). Functional imaging of the brain using computed tomography. *Radiology*, 138: 711-716.

Brandt-zawadski M and Norman D (1987). Magnetic Resonance Imaging of Central Nervous System. Raven Press, New York.

Brassow F and Baumann K (1978). Volume of brain ventricles in man determined by computer tomography. *Neuroradiology*, 16: 187-189.

Caird FI (1977). Computerized axial tomography for intracranial diagnosis. *Proc Aust Assoc Neurol*, 13: 24-29.

Celik HH, Gurbuz F, Erilmaz M and Sancak B (1995). CT measurement of the normal brain ventricular system in 100 adults. *Kaibogaku Zasshi*, 70: 107-115.

Chitkara U, Gogswell C, Norton K, Wilkins IA, Mehalek K and Berkowitz RL (1988). Choroid plexus cysts in the fetus: A benign anatomic variant or pathologic entity? Report of 41 cases and review of the literature. *Obstet Gynecol*, 72: 185-189.

Cohen BM, Buonanno F, Keck PE Jr, Finklestein SP and Benes FM (1988). Comparison of MRI and CT scans in a group of psychiatric patients. *Am J Psychiatry*, 145: 1084-1088.

Goldstein I, Reece A, Luigi-pilu G, Jobbins J and Bovicelli I (1988). Sonographic evaluation of the normal developmental anatomy of the fetal cerebral ventricles: I. The frontal horn. *Obstet Gynecol*, 72: 588-592.

Cramer GD, Allen DJ, Didio LJ, Potvin W and Brinker R (1990). Comparison of computerized tomography with magnetic resonance imaging (MRI) in the evaluation of encephalic ventricular volume. *Surg Radiol Anat*, 12: 135-141.

Cremin BJ, Chilton SJ and Peacok WJ (1983). Anatomical landmarks in anterior fontanelle ultrasonography. *Br J Radiol*, 56: 517-526.

DeCarli C, Maisog J, Murphy DG, Teichberg D, Rapoport SI and Horwitz B (1992). Method for quantification of brain, ventricular and subarachnoid CSF volumes from MR images. *J Comput Assit Tomogr*, 16: 274-284.

Denkhaus H and Winsberg F (1979). Ultrasonic measurement of the fetal ventricular systems. *Radiology*, 131: 781-786.

Dewbury KC and Bates RI (1981). The value of transfontanellar ultrasound in infants. *Br J Radiol*, 54: 1044-1050.

Ellington M, Babcok DS and Han BK (1982). Technical considerations in imaging the infant head by ultrasonography. *Sem Ultrasound*, 3: 182-190.

Evens RG (1976). New frontier for radiology: computed tomography. *Am J Roentgenol*, 126: 1117-1129.

Fleckenstein P and Jensen JT (1995). Bases anatómicas del diagnóstico por la imagen. Mosby Doyma Libros, Madrid.

Gilmore JH, Gerig G, Specter B, Charles HC, Wilber JS, Hertzberg BS and Kliewer MA (2001). Infant cerebral ventricle volume: a comparison of 3-D ultrasound and magnetic resonance imaging. *Ultrasound Med Biol*, 27: 1143-1146.

Goldstein SJ, Lee C and Rosenbaum HD (1986). Magnetic resonance and computed tomographic imaging of mass lesions of the cerebral ventricles. A prospective comparative study. *Acta Radiol Suppl* 369: 186-189.

Grant EG, Schellinger D, Borts FT, McCullough DC, Friedman GR, Sivasubramanian KN and Smith Y (1981). Real-time sonography of the neonatal and infant head. *Am J Radiol*, 136: 265-271.

Gualdi GF, Trasimeni G, Di Biasi C, Iannilli M, Polettini E, Melone A, Volpe A and D'amico D (1993). Computerized tomography and magnetic resonance in the evaluation of neoplastic processes localized on the floor of the third ventricle. *Clin Ter*, 143: 57-65.

Gualdi GF, Di-biasi C, Trasimeni G, Iannilli M, Polettini E, Melone A, Volpe A and D'amico D (1993). Diagnostic imaging in the evaluation of mases developing in the cerebral ventricles. *Clin Ter*, 142: 361-368.

Gyldensted C and Kosteljanetz M (1976). Measurements of the normal ventricular system with computer tomography of the brain. A preliminary study on 44 adults. *Neuroradiology*, 10: 205-213.

Hagen-ansert SL (1989). Textbook of diagnostic ultrasonography. CV Mosby Company, Saint Louis.

Huckman MS, Grainer LS and Clasen RS (1977). El tomograma computarizado normal. *Seminarios de Roentgenología*, 12: 38-60.

JEANTY P, DRAMAIX-WILMET M, DELBEKE D, RODESCH F and STRUYVEN H (1981). Ultrasonic evaluation of ventricular growth. *Neuroradiology*, 21: 127-131.

JERNIGAN TL, ZATZ LM, MOSES JA Jr and BERGER PA (1982). Computed tomography in schizophrenics and normal volunteers. I. Fluid volume. *Arch Gen Psychiatry*, 39: 765-770.

JACOBSON HG (1987). Fundamentals of magnetic resonance imaging. *JAMA*, 258: 3417.

JOHNSON LA, PEARLMAN JD, MILLER CA, YOUNG TI and THULBORN KR (1993). MR quantification of cerebral ventricular volume using a semiautomated algorithm. *Am J Neuroradiol*, 14: 1373-1378.

KEAN DM and SMITH MA (1986). Magnetic resonance imaging: principles and applications. Williams & Wilkins Co., Baltimore.

KESHAVAN MS, ANDERSON S, BECKWITH C, NASH K, PETTEGREW JW and KRISHNAN KR (1995). A comparison of stereology and segmentation techniques for volumetric measurements of lateral ventricles in magnetic resonance imaging. *Psychiatry Res*, 61: 53-60.

KIRKWOOD JD (1990). Essentials of neuroimaging. Churchill Livingstone, New York.

KREMKAU FW (1980). Diagnostic ultrasound. Physical principles and exercises. Grune & Stratton, New York.

KROFT CL, GESCUK B, WOODS BT, MELLO NK, WEISS RD and MENDELSON JH (1991). Brain ventricular size in female alcoholics: an MRI study. *Alcohol*, 8: 31-34.

LANKSCH W and KAZNER E (1976). Cranial computerized tomography. Springer, Berlin.

LEIRA HL, MYHR G, NILSEN G and DALE LG (1992). Cerebral magnetic resonance imaging and cerebral computerized tomography for patients with solvent-induced encephalopathy. *Scand J Work Environ Health*, 18: 68-70.

LÓPEZ OL, BECKER JT, JUNGREIS CA, REZEK D, ESTOL C, BOLLER F and DEKOSKY ST (1995). Computed tomography-but not magnetic resonance imaging-identified periventricular white-matter lesions predict symptomatic cerebrovascular disease in probable Alzheimer's disease. *Arch Neurol*, 52: 659-664.

MANCUSO AA and HANAFEE WN (1985). Computed tomography and magnetic resonance. Imaging of the Head and Neck. 2nd ed. Williams and Wilkins, Baltimore.

MATSUMAE M, KIKINIS R, MOROCZ I, LORENZO AV, ALBERT MS, BLACK PM and JOLESZ FA (1996). Intracranial compartment volumes in patients with enlarged ventricles assessed by magnetic resonance-based image processing. *J Neurosurg*; 84: 972-981.

MIRVIS SE (1989). Applications of magnetic resonance imaging and three-dimensional computed tomography in emergency medicine. *Ann Emerg Med*, 18: 1315-1321.

MUÑOZ GONZÁLEZ A, GÓMEZ GONZÁLEZ J and ROSEN B (1989). Indicaciones neurológicas actuales de la resonancia magnética (I). *Med Clin*, 92: 421-428.

NAIDICH TP, TEETER BC, NIEVES A, CRAWFORD CR, PRENGER E and MCLONE DG (1989). Rapid three-dimensional display of the cerebral ventricles from noncontrast CT scans. *J Comput Assist Tomogr*, 13: 779-788.

PAKKENBERG B, BOESEN J, ALBECK M and GJERRIS F (1989). Unbiased and efficient estimation of total ventricular volume of the brain obtained from CT-scans by a stereological method. *Neuroradiology*, 31: 413-437.

PENN RD, BELANGER MG and YASNOFF WA (1978). Ventricular volume in man computed from CAT scans. *Ann Neurol*, 3: 216-223.

PENTLOW KS, ROTTENBERG DA and DECK MD (1978). Partial volume summation: a simple approach to ventricular volume determination from CT. *Neuroradiology*, 16: 130-132.

PIGADAS A, THOMPSON JR and CRUBE GL (1981). Normal infant brain anatomy: correlated real-time sonograms and brain specimens. *Am J Radiol*, 137: 815-820.

RAZ S, RAZ N, WEINBERGER DR, BORONOW J, PICKAR D, BIGLER ED and TURKHEIMER E (1987). Morphological brain abnormalities in schizophrenia determined by computed tomography: a problem of measurement? *Psychiatry Res*, 22: 91-98.

ROTTENBERG DA, PENTLOW KS, DECK MD and ALLEN JC (1978). Determination of ventricular volume following metrizamide CT ventriculography. *Neuroradiology*, 16: 136-139.

SACHER M, GOTTESMAN RI, ROTHMAN AS, ROSENBLUM BR and HANDLER MS (1990). Magnetic resonance imaging and computed tomography of an intraventricular craniopharyngioma. *Clin Imaging*, 14: 116-119.

SEIDEL G, KAPS M, GERRIETS T and HUTZELMANN A (1995). Evaluation of the ventricular system in adults by transcranial duplex sonography. *J Neuroimaging*, 5: 105-108.

SHAH PS, SARVAIYA JB, RAWAL JR, KABRA SK, PATEL VB and JOSHI RN (1992). Normal ventricular size and ventriculohemispheric ratio in infants up to 6 months of age by cranial ultrasonography. *Indian Pediatr*, 29: 439-442.

STARK DD and BRADLEY WG (1987). Magnetic Resonance Imaging. Mosby, Chicago.

SYNEK V, REUBEN JR, GAWLER J and DU BOULAY GH (1979). Comparison of the measurements of the cerebral ventricles obtained by CT scanning and pneumoencephalography. *Neuroradiology*, 17: 149-151.

TANG Y, WHITMAN GT, LÓPEZ I and BALOH RW (2001). Brain volume changes on longitudinal magnetic resonance imaging in normal older people. *J Neuroimaging*, 11: 393-400.

WAHLUND LO (1996). Magnetic resonance imaging and computed tomography in Alzheimer's disease. *Acta Neurol Scand* Suppl 168: 50-53.

WALSER RL and ACKERMAN LV (1977). Determination of volume from computerized tomograms: finding the volume of fluid-filled brain cavities. *J Comput Assist Tomogr*, 1: 117-130.

YOUNG SW (1984). Magnetic Resonance Imaging Basis Principles. Raven Press, New York.

ZIPURSKY RB, LIM KO and PFEFFERBAUM A (1990). Volumetric assessment of cerebral asymmetry from CT scans. *Psychiatry Res*, 35: 71-89.